ELSEVIER

Journal of Nuclear Materials 266–269 (1999) 1–13

journal of nuclear materials

Section 1. Invited papers

D–T experiments in the JET tokamak

M. Keilhacker *, M.L. Watkins, JET Team

JET Joint Undertaking, Abingdon, Oxon, OX14 3EA, UK

Abstract

During the second half of 1997, JET carried out a broad-based series of D–T experiments (DTE1) producing a total of 675MJ of fusion energy. A large scale tritium supply and processing plant, the first of its kind, allowed the repeated use of the 20 g tritium on site, supplying a total of 99.3 g of tritium to the machine. After DTEl, the tritium inventory in the torus remained a factor of about three higher than expected from the Preliminary Tritium Experiment in 1991, and this is thought to be related to tritium-saturated carbon films on surfaces which are shadowed from erosion by the plasma. During DTE1 records were set for peak (16.l MW) and quasi steady-state (4 MW for 4 s) fusion power and for the ratio of fusion power to input power (0.62; if a similar plasma could be obtained in steady-state, the Q would be 0.94 ± 0.17). Alpha particle heating was clearly demonstrated and shown to be consistent with classical expectations. In the optimised shear mode of operation internal transport barriers were established for the first time in D–T, with a threshold power roughly equal to that in D–D. ELMy H-mode studies in D–T have considerably strengthened the basis for predicting the heating requirements and performance of ITER. Candidate ICRF heating schemes for ITER were successfully tested and the relevant simulation codes validated. With regard to isotope effects in ELMy H-modes, the ITER scaling for the H-mode threshold power had to be modified to include an inverse mass dependence ($\approx A^{-1}$), while energy transport showed little dependence on isotope and seems to involve different physics in the edge and the core of the plasma. JET confinement data obtained under conditions which were identical to ITER in most dimensionless parameters scale close to gyro-Bohm and predict ignition for ITER provided the required densities can be reached.

Keywords: JET; Tritium inventory; Tritium inventory; Fusion; Divertor; Tokamak

1. Introduction

The first ever significant amount of controlled fusion power was produced in the Preliminary Tritium Experiment (PTE) in the Joint European Torus (JET) on 9 November 1991 [1], when a plasma containing 11% of tritium in deuterium produced a peak fusion power of 1.7 MW averaging 1 MW for 2 s and a fusion gain $P_{\text{fusion}}/P_{\text{in}} = 0.12$. These plasmas were terminated by magnetohydrodynamic events which led to overheating of the target plates and resulting in large influxes of carbon (carbon 'bloom'). Since then, JET has installed a sequence of progressively more closed divertors. The present Mark IIA divertor [2] is very effective at accepting heat loads from the plasma, and large impurity influxes no longer occur. In the period from 1993 to 1997, the Tokamak Fusion Test Reactor (TFTR) operated with deuterium–tritium (D–T) mixtures and, using the optimum mixture, has produced 10.7 MW of fusion power and $P_{\text{fusion}}/P_{\text{in}} = 0.27$ [3].

JET is closest in scale and plasma parameters to the International Thermonuclear Experimental Reactor (ITER) [4], has an ITER-like divertor configuration (bottom single null) and can be operated in the standard operating mode foreseen for ITER, the H-mode with Edge Localised Modes (ELMs). Consequently, JET carried out a broad based series of D–T experiments (DTE1) in 1997 to address crucial issues of D–T technology and physics for ITER.

The physics objectives of DTE1 can broadly be divided into two areas, high fusion performance and ITER physics in D–T. The fusion performance programme [5]

* Corresponding author. Tel.: +44-1235 464 554; fax: +44-1235 464 465

0022-3115/99/$ – see front matter
PII: S0022-3115(98)00811-3

had the major aims to obtain high fusion power and Q in three JET operating modes, the hot ion ELM-free H-mode, the optimised shear mode and the steady state ELMy H-mode, and to demonstrate alpha particle heating. The main aims of the ITER physics programme [6] were to study, under ELMy H-mode conditions, the isotope effects on global energy confinement and H-mode threshold power and to evaluate ion cyclotron resonance frequency heating schemes in D–T.

All these objectives had to be met within a strict budget of 2.5×10^{20} neutrons. This limit was set so that the resultant activation of the JET vessel would not prevent manned in-vessel intervention for more than a year after the end of DTE1.

In addition, DTE1 had a technology mission, namely to demonstrate an ITER scale tritium processing plant operating closely coupled to a tokamak, and to carry out, following DTE1, an exchange of the divertor target structure exclusively by remote handling.

Following the D–T experiments the JET experimental programme continued for about two months with specific ITER physics studies in hydrogen ('isotope effect') and deuterium, before the remote handling shutdown for the exchange of the divertor target started.

In this paper an overview of the most significant results from DTE1 (first results were reported in [7]) and – where appropriate – the specific ITER physics campaign is given, and the implications of these results for ITER and a reactor are pointed out. First tritium supply, processing, plasma concentrations and wall retention are discussed (Section 2). Then high fusion performance and alpha particle heating in ELM-free H-mode plasmas (Section 3) and the development of the optimised shear regime in D–T (Section 4) are addressed. This is followed by a discussion of ICRF heating (Section 5) and of the confinement and threshold power (Section 6) of ITER ELMy H-mode plasmas in D–T. Section 7, finally, deals with the remote handling exchange of the divertor target structure. The first and last Sections address technology issues and Sections 3–6 physics issues.

2. Tritium supply, processing, plasma concentrations and wall inventory

2.1. Tritium supply and processing

During DTE1, 20 g of tritium were stored on the JET site in U-beds, and transferred using cryo-transfer systems. The tritium was supplied, collected from the exhaust gases and reprocessed by an industrial scale tritium processing plant which worked in a closed-cycle with the tokamak, pumping the torus in continuous operation. In all, 99.3 g of tritium was supplied to the JET machine, requiring eight processing cycles in which the tritium was routinely separated to better than 99.5% purity. The tritium gas was either injected directly into the torus via a gas valve (a total of 35 g) or by Neutral Beam (NB) injection. For this purpose, one of the two NB injectors was operated with up to 100% tritium, delivering 11 MW at 160 keV. In this case the tritium gas was supplied to the NB box and a small fraction was then injected into the torus via the high energy tritium neutral beams. The remaining tritium gas was trapped by the NB cryopumps and was retrieved in nightly regenerations.

2.2. Tritium plasma concentrations and wall inventory

One of the first experiences of DTE1 was that the tritium concentrations in the plasma could be relatively easily controlled by loading the walls to an appropriate level of tritium using ohmic or low power ICRF heated discharges. Later during DTE1, valuable information for ITER was obtained on wall inventory and clean up methods [8].

As shown in Fig. 1(a), which compares the measured tritium concentrations during DTE1 with a prediction based on the experience from the PTE, tritium concentrations in the plasma and exhaust gases were reduced at a rate similar to that in the PTE. However, as shown in Fig. 1(b), the tritium inventory developed quite differently during DTE1 compared to the PTE: during DTE1 the torus consumed $\approx$30% of the tritium introduced. This level was reduced to $\approx$17% following extensive operation in hydrogen and deuterium. Even at the end of this clean-up phase, the tritium inventory was still much higher than expected from an extrapolation based on the PTE tritium retention. These observations suggest a non-recoverable sink for tritium which was not present in the PTE. Such a sink has been identified in the form of deuterium-saturated carbon films and flakes on surfaces which are shadowed from erosion by the plasma and are too cold to outgas. As discussed in [8], the high levels of tritium retention observed in JET would be unacceptablely high for ITER, and the ITER divertor needs to be re-designed to take this fully into account.

3. High fusion performance and alpha particle heating

3.1. High fusion performance

The ELM-free H-mode was the work horse for high performance operation during DTE1, producing record fusion power and Q. In addition, notable physics results were obtained in this mode.

JET's experience over many years with ELM-free H-mode plasmas in deuterium [9] has shown that they exhibit high energy confinement, a neoclassical edge transport barrier with a loss power which scales as $n^2 Z_{\mathrm{eff}}/I$ [10], and are finally terminated by MHD events, particularly sawteeth, outer modes (external kink modes) and giant ELMs (ballooning modes). The operational

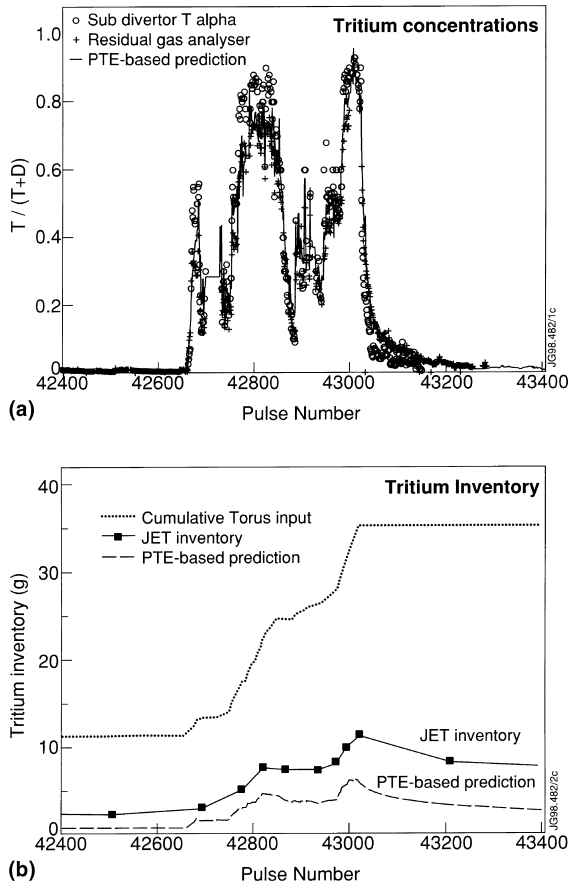

Fig. 1. (a) Tritium concentrations in the plasma and exhaust gases and (b) tritium inventory in the torus during DTEl (pulse Nos. 42661–43023) and comparison with predictions based on the PTE.

scenario developed, therefore, employs high plasma current and low recycling to maximise energy confinement, gas puffing to provoke an early sawtooth and to reduce Z_{eff} and current ramp down to ameliorate the outer mode (but at the expense of reducing confinement).

The first task in the D–T campaign was to clarify the relative contributions of NB fuelling and wall recycling to the plasma mix in the ELM-free H-mode regime. To this end, the NB mix was varied from pure deuterium to pure tritium whilst the walls were still predominantly deuterium. A comparison of these mixture control experiments with TRANSP predictions demonstrated that the contribution of wall/target recycling and gas puffing to the core fuelling was about twice as large as that from the NB fuelling. For the high power experiments, therefore, deuterium gas fuelling was replaced by mixed D–T fuelling and by loading the walls with an appropriate D–T mix.

In all, eight high power ELM-free H-mode pulses were produced in D–T, five of which delivered more than 12 MW of fusion power each. The highest performance was achieved in the pulses with the highest toroidal field (3.6 T) and plasma current (4.2 MA). Fig. 2 shows the pulse with the highest D–T fusion power of 16.1 MW (a similar pulse, one hour earlier and with 25.3 MW of additional heating, produced 15.8 MW of fusion power), which was obtained with 25.4 MW of additional heating using NB injection (22.3 MW) together with some hydrogen minority ICRF heating. In common with experience of deuterium operation in JET, the stored energy (not shown), fusion power and density (not shown) rise monotonically with time. The ion temperature levels off around 28 keV, significantly higher than the electron temperature which is about 14 keV. The ELM-free period is limited by MHD activity (as manifested in the structure of the Balmer Alpha trace): first an outer mode and then a giant ELM. Following detection of the giant ELM, the heating power is switched off to save neutrons. As shown in the bottom panel of Fig. 2, this pulse reaches $Q_{\text{in}} = P_{\text{fus}}/P_{\text{in}} = 0.62$ and a ratio of fusion power to net input power (P_{in} − dW/dt), $Q_{\text{tot}} = 0.94 \pm 0.17$ [5], the value which

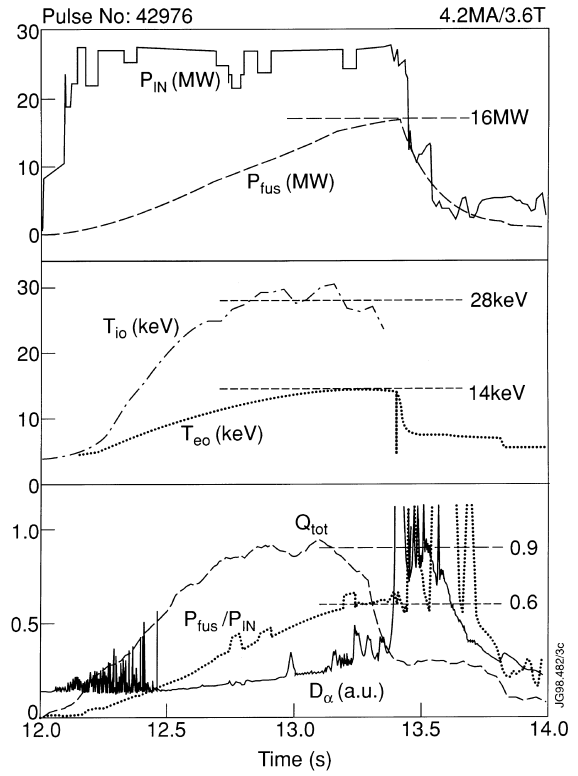

Fig. 2. Various time traces for the highest fusion yield hot ion H-mode discharge. From top to bottom: Input and fusion power; central ion and electron temperature; the quantity Q_{tot} defined in the text, the ratio of fusion power to input power and D_α/T_α intensity.

Q_{in} would reach if a similar plasma could be obtained in steady state.

Comparison of similar D–T and D–D discharges showed that the increase in fusion yield (about 88 times in neutron rate and 210 times in fusion power) agreed with that expected from the respective reaction rate coefficients.

No alpha particle driven Toroidal Alfvén Eigenmodes (TAEs) were excited in these high performance D–T discharges, even though TAEs had been observed under other circumstances in JET (e.g. with ICRF heating above a certain threshold power). This is in agreement with stability calculations which show that the normalised alpha particle pressure, β_α, of these discharges is a factor of two below the instability threshold [11].

3.2. Alpha particle heating

JET plasmas with the highest fusion performance have about 3 MW of alpha particle heating compared to a total input power of about 25 MW. Since the alpha particle heating is centrally peaked and couples mainly to the electrons, it should be observable, despite competition from other power inputs to the electrons.

To separate the alpha particle heating from possible isotope effects on energy confinement, a D–T mixture scan, in which the tritium concentration was varied from 0 to 90%, was carried out in otherwise similar discharges (3.8 MA/3.4 T) in which the external heating power was kept as constant as possible (≈10.5 MW NB heating) [12]. Comparing the pure deuterium and almost pure tritium ends of this scan demonstrated (lower panel of Fig. 3) that there is at most a very weak isotope dependence of global energy confinement in ELM-free H-modes. The slight increase in confinement in the centre of the scan is due to the peaked alpha power source which nearly doubled the power transferred to the electrons on axis. The strong correlation between the maximum diamagnetic and thermal plasma energies and the optimum D–T mixture (upper panel of Fig. 3), is a clear indication of alpha particle heating. This is even clearer from Fig. 4 which is a plot of the central electron temperature versus the calculated alpha particle heating power for the set of pulses in the D–T mixture scan. The highest electron temperature shows a clear correlation with the maximum alpha particle heating power and with the optimum D–T mixture (40:60). A regression fit to the data gives a change in central electron temperature of 1.3 ± 0.23 keV with 1.3 MW of alpha particle heating power.

These JET experiments are a clear demonstration of the self-heating of a D–T plasma by the alpha particles produced by fusion reactions. A comparison with ICRF heating of deuterium plasmas under similar conditions showed that the alpha particle heating was as effective as hydrogen minority ICRF heating (which, like the alpha

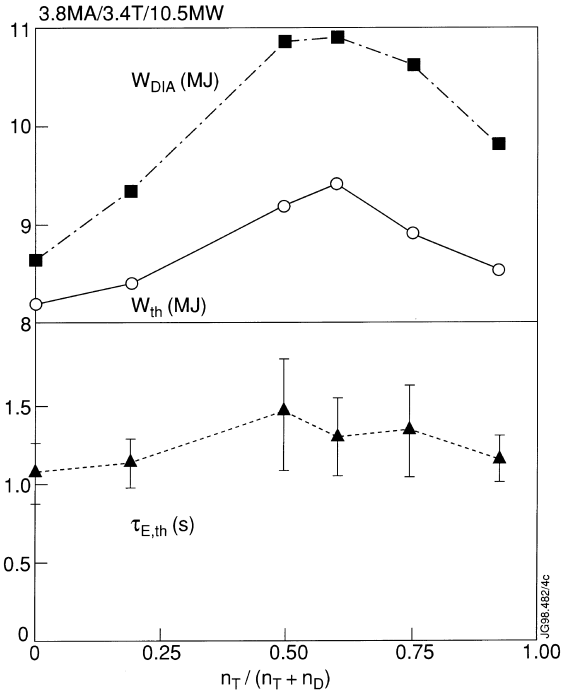

Fig. 3. Diamagnetic and thermal plasma energy contents (upper) and global energy confinement time (lower) versus D–T mixture.

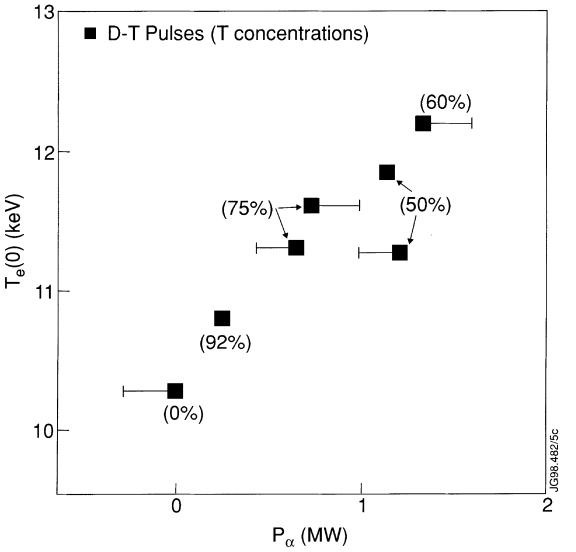

Fig. 4. Central electron temperature (from ECE) versus alpha particle heating power. The bars indicate the variation in NB power compared to the 92% tritium reference pulse. The figures in brackets are the tritium concentrations $n_T/(n_T + n_D)$.

particles, mainly heats the electrons). This is a strong indication that, at least in the absence of alpha particle driven TAE instabilities (see above), the trapping and slowing down of the alpha particles and the resulting heating are classical.

4. Development of the optimised shear regime in D–T

The advanced tokamak concept proposes the use of profile control techniques to engineer high plasma confinement and to develop these conditions into steady state. This concept, if successful, would give ignition and sustained burn at lower plasma current, thereby reducing the size and cost of a reactor. JET has been particularly suited to such studies by virtue of its combination of heating schemes and its current drive capability. In fact, JET reported the first observations of plasmas with reversed central magnetic shear and improved core confinement in the Pellet-Enhanced Performance (PEP) mode of 1988 [13,14]. Similar reversed shear modes with reduced transport in the plasma core were then also developed on DIII-D [15], TFTR [16] and JT-60 [17]. More recently, JET returned to this mode of operation, developing an optimised shear scenario [18] in which pressure profiles are more peaked and D–D neutron yields are higher than in the ELM-free H-mode.

A key element in these scenarios is the formation of an Internal Transport Barrier (ITB) and these have now been established for the first time in D–T (Fig. 5). Power and current profile control are used to establish an ITB, to delay the transition to an H-mode phase, and to avoid a β-limit disruption. The scenario comprises the formation of a target plasma by pre-heating during a fast current ramp with a combination of lower hybrid waves to assist breakdown and provide some current drive. This is followed by ICRF pre-heating to arrest current penetration. When the current profile is such that the volume within the $q=2$ surface is reasonably large ($r/a \approx 0.3$–0.4), the full heating power, typically 16–18 MW of NB heating together with 6 MW of ICRF heating, is applied. In D–D the highest fusion performance was obtained when a clear H-mode transition was delayed for as long as possible. This was achieved by using a low target density, strong divertor pumping, a low triangularity configuration and by maintaining the current ramp throughout the main heating phase. When an ITB is established, the resulting good core confinement maintains the plasma loss power below the level required to trigger an H-mode, thus preserving an L-mode edge.

In D–T, the scenario had to be modified, largely because of the lower H-mode threshold power. However, after some scenario development, strong ITBs were established for the first time in D–T plasmas, and with similar additional heating power levels and current profiles to those in D–D [19]. In D–T, as in D–D, the

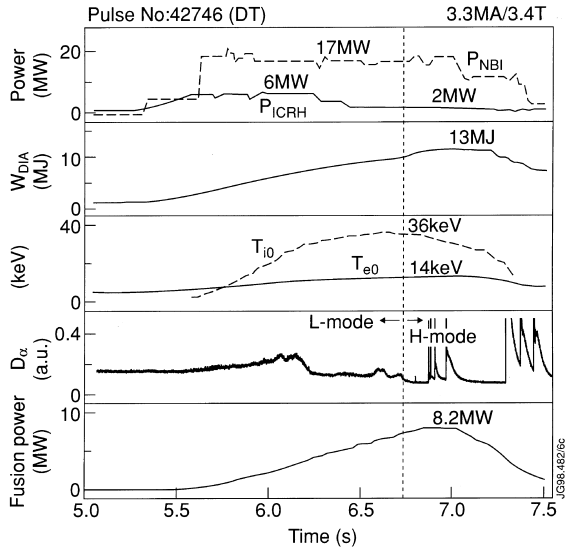

Fig. 5. Various time traces for the optimised shear discharge with the highest fusion yield. From top to bottom: NB and ICRF input power; diamagnetic energy; central ion and electron temperatures; D_α/T_α intensity; and fusion power.

foot of the steep gradient region is positioned just inside the $q=2$ surface and both move outwards with time.

When an ITB forms, substantial increases in plasma density and temperature (Fig. 6) occur during the first second of high power heating. As shown in Fig. 6, the temperature gradient can reach 150 keV/m and the pressure gradient 1 MPa/m. The input power is controlled by feedback on the neutron rate in order to avoid excessive pressure gradients which provoke MHD in-

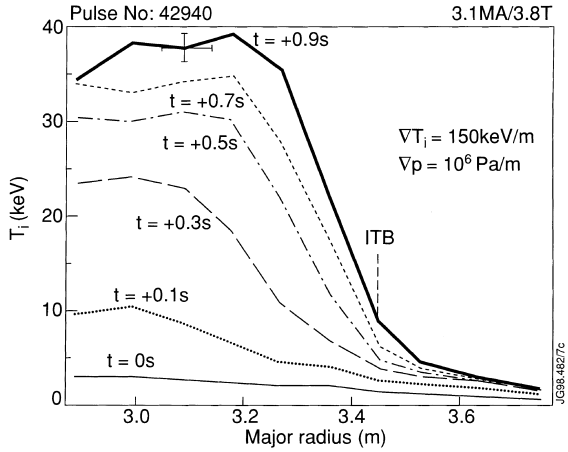

Fig. 6. Ion temperature profiles at various times following the application of high power heating in an optimised shear discharge in D–T showing the formation of an internal transport barrier (ITB).

stabilities. As a result, the plasma can be maintained close to the ideal MHD stability limits for most of the heating pulse, as shown in Fig. 7 for optimised shear discharges in D–D and in D–T. In both cases, β_N increases as the ITB moves outwards with time to ≈2/3 of the plasma radius and the pressure profile becomes less peaked. Towards the end of the discharge, an H-mode forms, reducing further the peaking factor, moving the discharge away from the instability boundary, but also leading to the subsequent termination of the discharge by disruption. The highest performance has been achieved with small or slightly reversed central shear and $q(0)$ in the range 1.5–2.

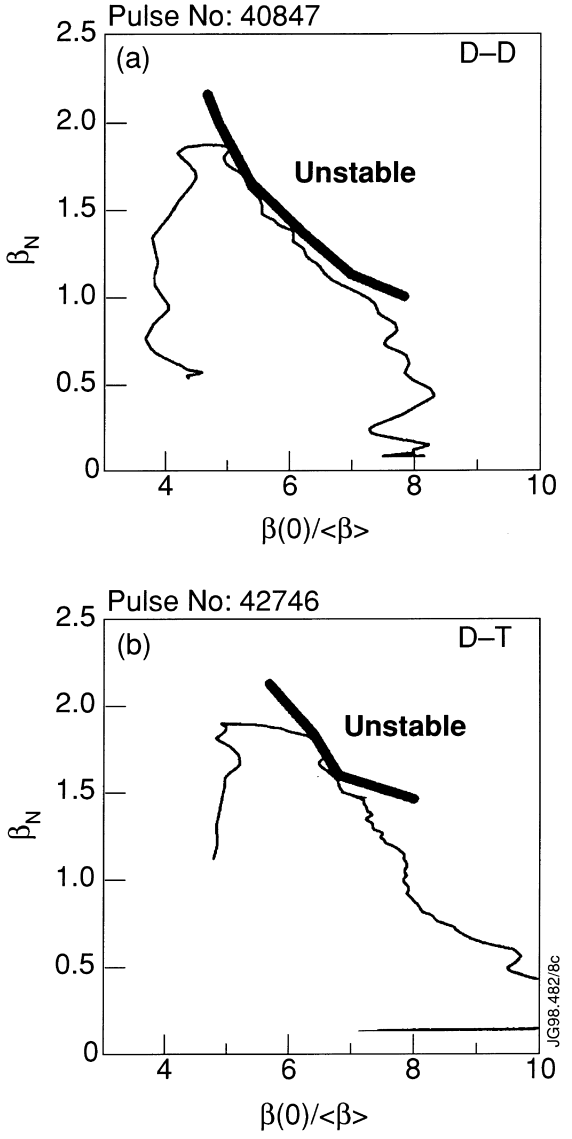

Fig. 7. Stability diagrams for two optimised shear discharges, (a) in D–D and (b) in D–T.

This behaviour is confirmed by TRANSP simulations, which also show that 2/3 of the neutrons were thermal in origin and that more than half of the full plasma current at peak performance was driven non-inductively, with the bootstrap and NB driven currents being about equal and localised close to the centre. Furthermore, the TRANSP calculations show that the ion thermal diffusivity can be very low and close to neoclassical levels within the ITB (Fig. 8).

The neutron and time constraints on DTE1 did not allow these discharges to be optimised. Nevertheless, 8.2 MW of fusion power was produced (Fig. 5), even though the tritium concentration (≈30%) and central density (4×10^{19} m^{-3}) were relatively low and the ion temperature (≈40 keV) was high. In fact, time-dependent transport code and stability calculations which have been calibrated against existing optimised shear discharges in JET and Tore Supra show that significant performance improvements are possible in JET.

These projections, in which the thermal fusion power was scaled from existing pulses as β_N^2 and the non-thermal fusion power was scaled proportional to the NB heating power, predict for operation at a magnetic field of 4 T a fusion power of up to 38 MW and a fusion $Q = P_{fus}/P_{in} = 1.5$ with the existing heating and current drive systems, and even higher fusion powers with modest upgrades (Fig. 9). The curves for β_N in Fig. 9 have been obtained from calculations with the JETTO transport code in which experimental data of the JET D–T pulse No. 42426 has been used as initial input. The predictive calculations apply a recently developed Bohm/gyro-Bohm transport model [20], which was validated on JET optimised shear discharges. In the calculations, current profile control with off-axis LHCD is

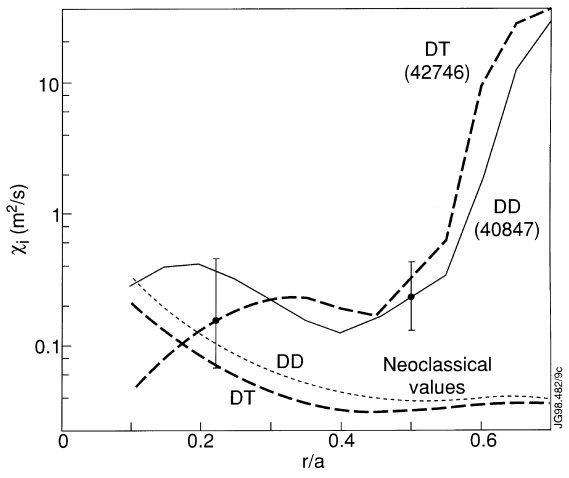

Fig. 8. Ion thermal diffusivities versus normalised plasma radius for two optimised shear discharges, one in D–D and the other in D–T, and comparisons with neoclassical values.

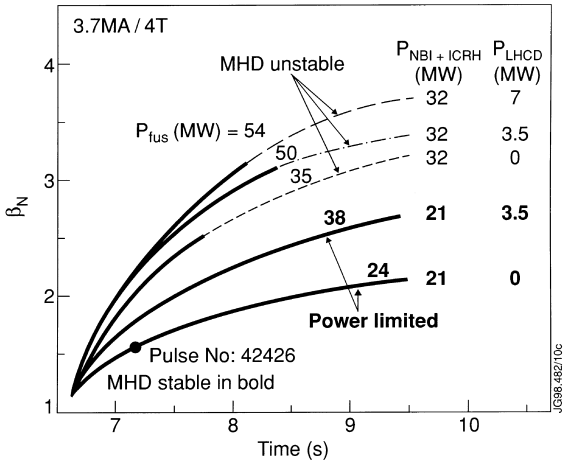

Fig. 9. Transport and stability predictions of the performance of optimised shear discharges in D–T at 4T with the present heating and current drive capabilities and with modest upgrades.

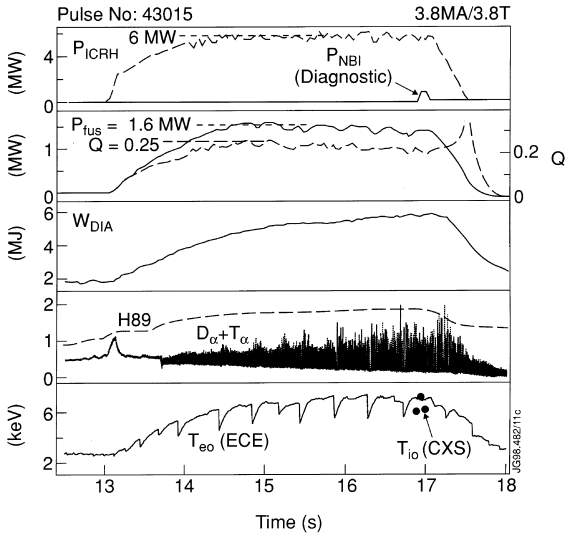

Fig. 10. H-mode plasma in which 6 MW of D(T) ICRH power gave 1.6 MW of fusion power and $Q = 0.22$ in quasi steady-state.

applied. The resulting widening of the low magnetic shear region leads to an expansion of the Internal Transport Barrier. The pressure profiles remain similar in shape to the experimental profiles, except in the outermost part of the steep gradient region. The wider core region of improved confinement and the higher central pressure give a considerable increase in β_N. The results of the transport calculations have subsequently been analysed with an MHD code [21] for stability.

5. ICRF heating of D–T plasmas

Ion cyclotron resonance frequency (ICRF) heating is one of the main heating methods foreseen for ITER and during DTE1 the physics and performance of the ICRF candidate schemes were tested successfully in D–T [22].

5.1. Deuterium minority heating, (D)T, at the fundamental resonance

In the case of deuterium minority heating at the fundamental resonance (ω_{cD}), the plasma density and the deuterium minority concentration (up to 15%) were optimised for maximum suprathermal fusion power which occurs for a deuterium energy of about 120 keV. This was also close to the critical energy so that optimum fusion reactivity with about equal bulk ion and electron heating was achieved. As shown in Fig. 10, a fusion power of 1.6 MW was produced with an ICRF input power of only 6 MW at 28 MHz in a 3.7 MA/3.7 T plasma with a species mix of ≈9% D and 91% T. A quasi steady-state fusion $Q = P_{fus}/P_{in} = 0.22$ was produced for almost 3 s, terminating only when the heating power was switched off. In this discharge, the central ion temperature reached 6.6 keV (measured by charge exchange spectroscopy using a NB 'blip') and the central electron temperature reached 7.2 keV. In discharges with lower density but higher deuterium concentration, the central ion and electron temperatures reached 10 keV and 8 keV, respectively.

5.2. ^{3}He minority heating, (^{3}He)D–T, at the fundamental resonance

With small amounts (>2%) of ^{3}He minority, ion absorption dominates (as in hydrogen minority heating in a deuterium plasma) and a significant ^{3}He tail is produced. By increasing the ^{3}He concentration to a level of 5–10%, the ^{3}He tail can be lowered sufficiently to produce strong bulk ion heating. As shown in Fig. 11, ^{3}He minority heating at the fundamental resonance (ω_c ^{3}He), produced the strongest heating with central ion and electron temperatures reaching 13 keV.

5.3. Second harmonic heating of tritium

In the case of heating at the second harmonic of tritium in a 50:50 D–T plasma (2 ω_{cT}), even at high plasma density the energy of the triton tails could not be lowered sufficiently, resulting in mainly electron heating (Fig. 11). The fusion power was mainly due to thermal reactions and was typically a factor of six less than with ^{3}He minority heating under similar conditions. However, code calculations for ITER, where the power

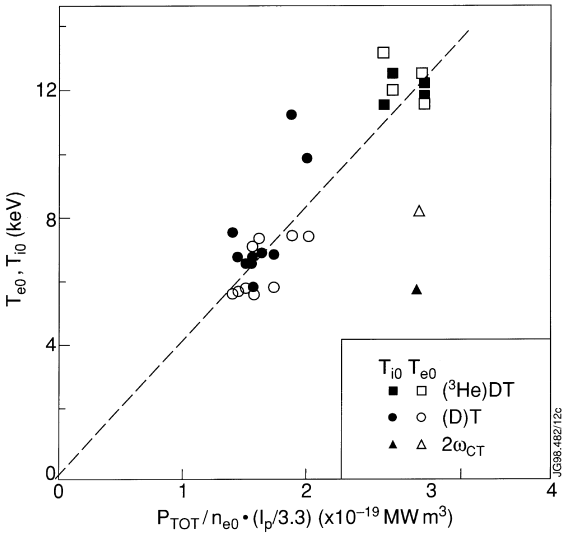

Fig. 11. Central ion and electron temperatures plotted against power per particle, corrected for values of plasma current different to 3.3 MA.

density per particle would be significantly lower, show that, under these conditions, this scheme would produce less energetic triton tails and mainly ion heating.

5.4. Code calculations and predictions for ITER

The experimental results are in excellent agreement with PION code calculations. The energy transfer rates to ions and electrons, as calculated by the PION code, predict strong ion heating for the deuterium and ^{3}He minority schemes, and mainly electron heating for the second harmonic tritium scheme, as observed in the experiments. The calculated neutron emission and the fast ion energy content for both the deuterium minority and the second harmonic tritium experiments are also in excellent agreement with observed reaction rates. These results give confidence in the use of such code calculations for predicting ICRF heating in future machines. For ITER they predict around 70% bulk ion heating on the route to ignition for the ^{3}He minority (with only 2.5% ^{3}He) scheme [23]. As heating progresses, the ^{3}He concentration can be reduced further and the scenario changes to 2 ω_{cT}.

6. Threshold power and confinement in ITER ELMy H-modes

6.1. Mass scaling of threshold power

The JET H-mode threshold power data base has been extended in deuterium to 4.2 MA/3.8 T, and now includes discharges with ≈60% and ≈90% tritium concentrations. The most notable result was that, in comparison with previous experiments in pure deuterium, the heating power needed to access the H-mode was lower in D–T and lower still in pure tritium, roughly as the inverse of the atomic mass (A^{-1}). This was first noted by observing the onset of ELMs in the Balmer Alpha light emission as the ICRF heating power was slowly ramped up over a 3 s period. The H-mode threshold power clearly decreased with increasing tritium concentration. The same threshold values were found with NB heated discharges.

In Fig. 12 the loss power from the plasma is plotted as a function of the scaling $P_{Th} = 0.76\ \bar{n}_e^{0.75}\ B\ R^2\ A^{-1}$, modified from that used for ITER [24] by inclusion of an inverse mass dependence; the constant has been adjusted to give the best fit to these JET data. Following DTE1, similar experiments were carried out in hydrogen, and these data are also shown in Fig. 12, confirming the strong inverse mass dependence. This has significant implications for ITER since it predicts a 33% reduction in the power needed to access the H-mode in a pure tritium plasma (for example, during the start-up phase when it is important to achieve high confinement in the H-mode regime as early as possible) and a 20% reduction in the power needed to maintain such conditions during high fusion power operation. As a result, the operational flexibility of ITER is increased.

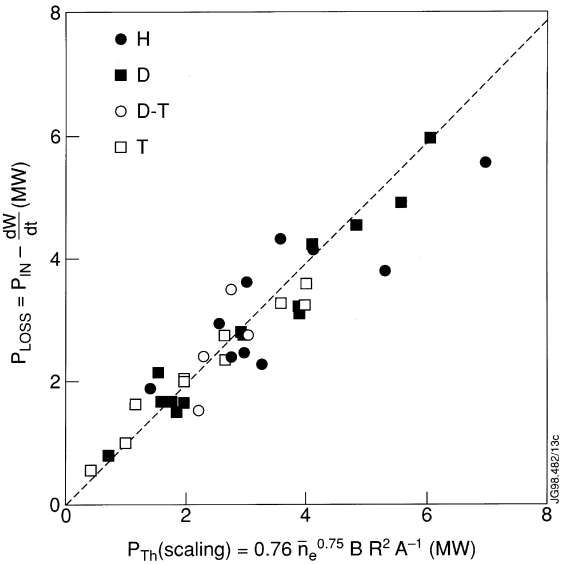

Fig. 12. Plasma loss power for ELMy H-mode discharges in hydrogen, deuterium, deuterium–tritium and tritium plotted against the ITER scaling for the H-mode threshold power modified to include an inverse mass dependence.

6.2. Edge operational space

The edge parameters of electron density, n_e (from the outer channel of the FIR interferometer), and temperature, T_e (from ECE measurements), in steady state ELMy H-modes show a cyclic behaviour during Type I ELMs and do not exhibit hysteresis between the L → H and H → L transitions. Furthermore, the superposition of (n_e, T_e) trajectories for discharges with increasing deuterium gas puffing rates defines an upper boundary in edge parameters for Type I ELMs which is best fitted by $T_e = 2.8 \times 10^{29}/n_e^{4/3}$ (eV, m^{-3}) [25].

Fig. 13(a) shows an example of the edge operating space in which the edge pressure is limited, as shown by the solid line for deuterium plasmas at 1.7 MA with 10–12 MW of NB heating. This result can be interpreted as a limit of the edge pressure gradient at the ideal ballooning limit, with the gradient region extending over a width which depends on an ion poloidal Larmor radius [25]. The edge parameters for similar 1.7 MA NB heated discharges in hydrogen and tritium are also shown in Fig. 13(a), indicating that, in comparison with deuterium, the maximum pressure is lower in hydrogen and higher in tritium. Data at 2.5 MA in deuterium and tritium are also shown, but scaled to 1.7 MA assuming that the pressure follows an I^2 dependence as might be expected from a limit due to ballooning modes.

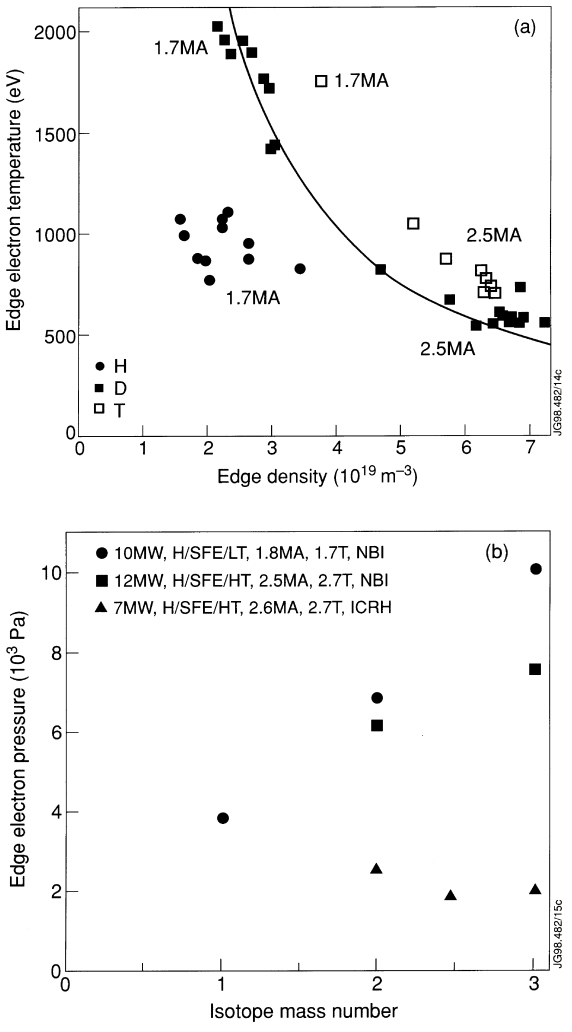

Fig. 13. (a) Operating space for edge electron density and temperature and (b) edge electron pressure for ELMy H-mode discharges in hydrogen, deuterium and tritium (the solid line corresponds to a pressure limited by ballooning modes over an ion poloidal Larmor radius).

A comparison of the upper boundary in edge parameters for Type I ELMs in similar NB heated discharges in hydrogen, deuterium and tritium shows that the maximum edge pedestal pressure increases with isotope mass (Fig. 13(b)). On the other hand, with ICRF heating of a hydrogen minority species, the pedestal pressure is observed to be lower, the amplitude of the ELMs is smaller and there is little dependence of the edge electron pressure on plasma species. This result with ICRF heating would be consistent with that obtained with NB heating if the ion Larmor scale length of the gradient region were that of the fast ions, rather than the thermal ions [26].

6.3. Mass scaling of global energy confinement

The scaling of the thermal energy confinement τ_{th} with the isotope mass, A, has been studied extensively on many devices using mainly hydrogen and deuterium isotopes [27–30]. More recently studies were completed in TFTR [31] with mixtures of deuterium and tritium in a variety of pulse types. For all pulse types the confinement increased with isotope mass $\tau_{th} \propto A^{\alpha}$ with α ranging from 0 to 0.85, in conflict with simple theoretical expectations, from which one would expect a small negative value for gyro-Bohm turbulence ($\alpha = 0.2$) and $\alpha = 0$ for long wavelength turbulence of the Bohm type.

During DTE1, steady state ELMy H-modes were obtained for a wide range of plasma currents (1–4.5 MA) and toroidal magnetic fields (1–3.8 T) in a 50:50 D–T mixture. The energy confinement times in these discharges were found to be consistent with the ITERH-EPS97(y) scaling [32] which is used at present for extrapolation to ITER.

The more complete data set for the steady state ELMy H-mode including deuterium, D–T and tritium discharges can also be fitted with the $A^{0.2}$ dependence of the ITERH-EPS97(y) scaling (Fig. 14), but a weaker mass dependence ($A^{0.03 \pm 0.1}$) fits better. This result may be considered in terms of a pedestal energy (defined as $3n_e(R_{edge})\ T_e(R_{edge})\ V$, where $R_{edge} \approx 3.8$ m, V is the plasma volume within R_{edge} and $T_i(R_{edge})$ is assumed to

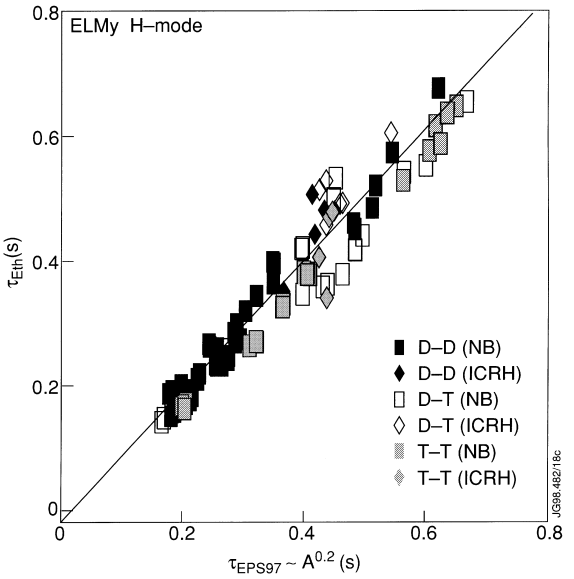

Fig. 14. Measured thermal energy confinement times in deuterium, deuterium–tritium and tritium ELMy H-mode discharges plotted against the ITER scaling law.

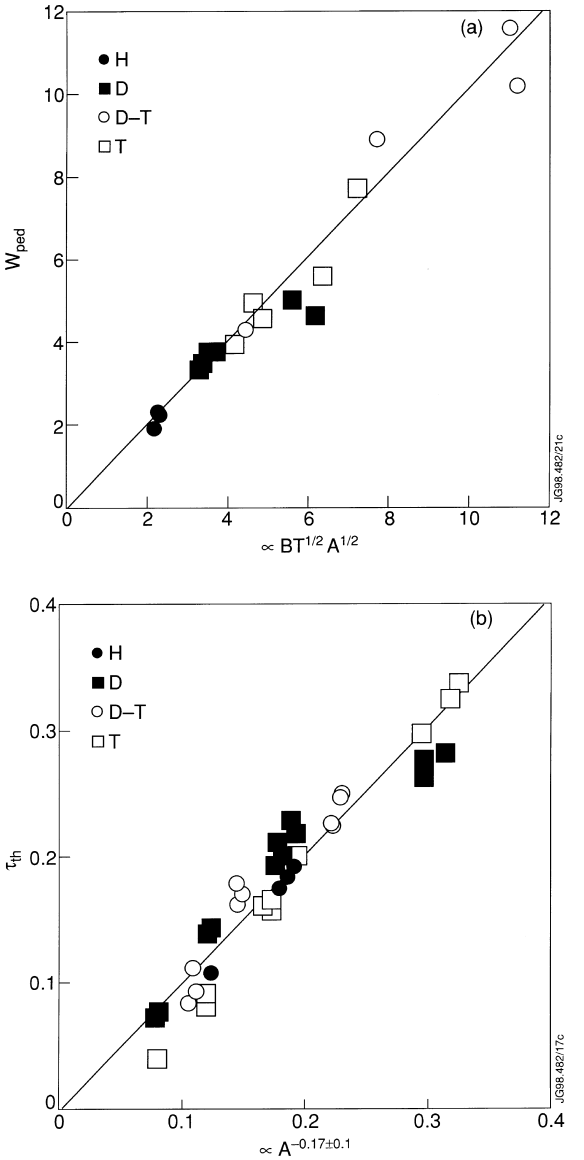

Fig. 15. (a) Pedestal energy plotted against that expected from an edge pressure gradient limited by ballooning modes over an ion poloidal Larmor radius and (b) the thermal confinement time of the core plasma plotted against the best fit for the mass dependence in a pure gyro-Bohm scaling for ELMy H-mode discharges in hydrogen, deuterium, deuterium–tritium and tritium.

be equal to $T_e(R_{edge})$, Fig. 15(a)) which could have a strong mass dependence ($A^{0.5}$ would result from the ballooning limit to the pressure gradient over a Larmor radius) and a core energy (determined by subtracting the pedestal energy from the total thermal energy, Fig. 15(b)), which, when divided by the net input power to the plasma, results in a gyro-Bohm mass dependence for the core energy confinement time ($A^{-0.2}$). This emphasises the importance of JET results for separating out edge effects in the global energy balance and for extrapolations to ITER.

6.4. Fusion performance in the ELMy H-mode regime

During DTE1 the best ever fusion performance in an ITER-like steady state ELMy H-mode was achieved with the production of a world record fusion energy of 21.7 MJ (Fig. 16). Regular Type I ELMs kept the discharge (3.8 MA/3.8 T) in steady-state with the ratio of the fusion energy produced to the input energy being 0.18 over 3.5 s (≈8 energy confinement times) and with 4 MW of fusion power being maintained for ≈4 s. The performance was limited to $\beta_N = 1.3$ by the available additional heating power (23 MW of combined NB (90%) and ICRF (10%) heating).

6.5. Extrapolation of the ELMy H-mode performance to ITER

While the normalised plasma pressure was too low for these discharges to qualify as ITER demonstration pulses, at lower toroidal field and plasma current (e.g. at 2 MA/2 T) the normalised plasma pressure ($\beta_N = 2.2$) and collisionality of an ignited ITER were closely matched on JET, and the edge safety factor was also close to the ITER value ($q = 3.2$). A gyro-Bohm extrapolation of such an ITER demonstration pulse gives ignition at the 1.5 GW level (or $Q = 5$ for a Bohm

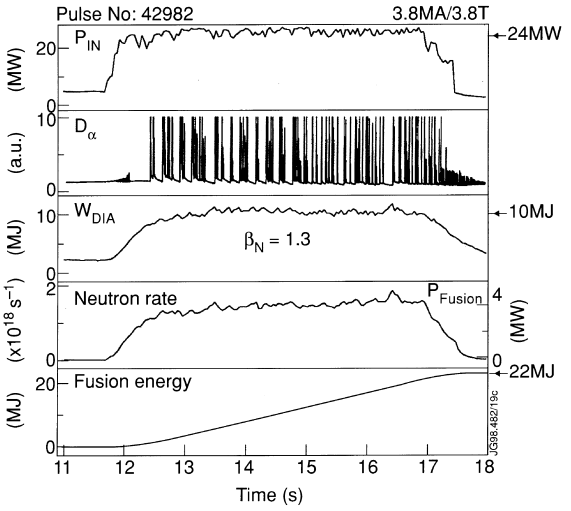

Fig. 16. Various time traces for the ELMy H-mode discharge with the highest fusion energy production. From top to bottom: total input power; D_α/T_α intensity; diamagnetic energy; neutron rate and fusion power; and fusion energy.

extrapolation) for ITER operating at 21 MA. The required density would, however, be about 50% above the Greenwald density [33], and it is assumed that this density can be reached without degrading confinement. On the other hand, for ITER operation at 24 MA, ignition at the 1.2 GW level is predicted for a gyro-Bohm extrapolation (or $Q = 10$ for a Bohm extrapolation), with the required density now being close to the Greenwald density.

7. Remote handling exchange of the divertor target

The shutdown for the remote handling exchange of the divertor target structure started in early February 1998 and will be completed by the end of May 1998. The main components of the remote handling equipment had been tested extensively in a full size torus mock-up and include [34]:

- A MASCOT two-armed, force-reflecting servo-manipulator with 20 kg capacity. The Mascot operates in a Master–Slave configuration with additional features for force scaling, gravity compensation and teach-repeat. The Mascot slave (Fig. 17) is configured with a miniature camera attached to each forearm and has a panorama/tilt camera and a 50 kg winch mounted between the shoulders;
- An articulated boom, 10 m long and with 180° torus reach, which can be pre-programmed;
- A tile carrier transfer facility comprising a short version of the articulated boom with a special end-effector designed to facilitate component transfer between the torus and special trolleys located in storage cabins; and
- A range of specially designed handling tools, wrenches and storage trays.

The methodology is based on a 'man-in-the-loop' strategy with coarse positioning operations carried out by computer teach files for the boom and final operations executed by a man using the force reflecting servo-system. This strategy allows checking and inspection of all planned operations and gives an intelligent response capability for unforeseen events.

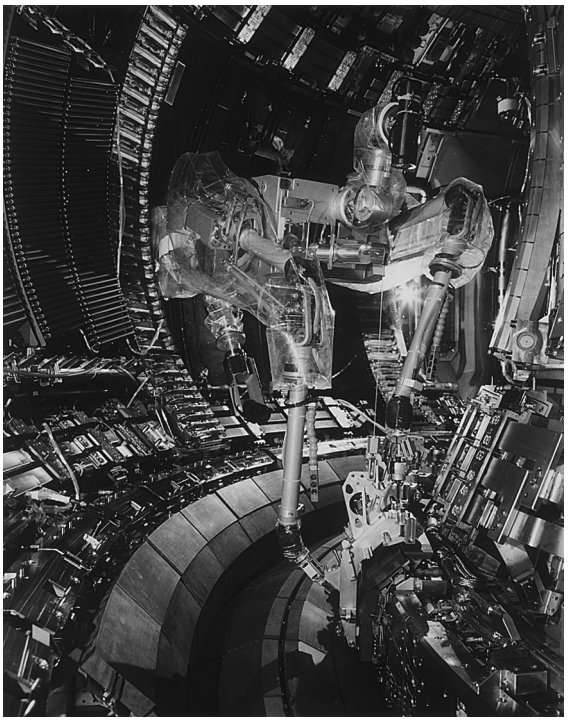

Fig. 17. The Mascot operating inside the JET torus.

8. Summary and conclusions

The D–T experiments on JET have been a tremendous scientific and technical success, producing unique and essential results for ITER.

In all, 675 MJ of fusion energy were produced during DTE1 and records were set for peak (16.1 MW) and quasi steady-state (4 MW for ≈4 s) fusion power and for the ratio of fusion power to input power (0.62; if a similar plasma could be obtained in steady-state, the Q would be 0.94 ± 0.17). Alpha particle heating was clearly demonstrated and shown to be consistent with classical expectations for trapping and slowing down of the alpha particles. In the optimised shear mode operation internal transport barriers were established for the

first time in D–T, and with a threshold power not markedly different from that in D–D. However, scaling information on the requirements for ITB formation is still lacking and several years of experiments will be required to create a data base as complete as that available at present for the ELMy H-mode. Full optimisation of the optimised shear mode was not possible within the constraints on DTE1, but model projections indicate that significant performance improvements leading to fusion powers above 20 MW and $Q > 1$ can be expected for the future.

The ELMy H-mode studies in D–T have considerably strengthened the basis for predicting the heating requirements and performance of ITER. Candidate ICRF heating schemes for ITER were successfully tested in D–T and the relevant simulation codes validated so that they now can be used with confidence for predicting ICRF heating in ITER. With regard to isotope effects in ELMy H-modes, the ITER scaling for the H-mode threshold power has to be modified to include an inverse mass dependence ($\approx A^{-1}$). This reduces considerably the power required for accessing and maintaining the H-mode and increases the operational flexibility of ITER. Energy transport shows little dependence on isotope and seems to involve different physics in the edge and the core of the plasma. JET confinement data obtained under conditions which are identical to ITER in most dimensionless parameters scale close to gyro-Bohm and point to ignition in ITER.

Finally, the control of the D–T mixture in the plasma proved to be relatively easy. Tritium concentrations in the plasma were reduced at a rate similar to that in the PTE but the tritium inventory in the torus remained a factor of about three higher than expected from the PTE. If this extrapolated to ITER, it would be unacceptable; modifications to the ITER divertor design would be required.

The fully remote replacement of the JET divertor target structure was completed successfully on 31 May 1998, a few days ahead of schedule. In two "unforeseen" events the system was able to prove its great adaptiveness and flexibility. This successful operation enhances the credibility of remote maintenance on future fusion devices. JET is now ready to restart operations with the more closed Mark IIGB divertor.

References

[1] JET Team, Nucl. Fusion 32 (1992) 187.
[2] JET Team, JET Progress Report 1997, JET Joint Undertaking, 1998, EUR 18199-EN-C (EUR-JET-PR15).
[3] K.M. McGuire et al., Proceedings of the 16th International Conference on Fusion Energy, Montreal, Canada, 1996, (IAEA, Vienna), Fusion Energy 1 (1997) 19.
[4] R. Aymar, V. Chuyanov, M. Huguet, R. Parker, Y. Shimamura, the ITER Joint Central Team and Home Teams, Proceedings of the 16th International Conference on Fusion Energy, Montreal, Canada, 1996, (IAEA, Vienna), Fusion Energy 1 (1997) 3.
[5] M. Keilhacker et al., the JET Team, High fusion performance from deuterium–tritium plasmas in JET, accepted for publication in Nucl. Fusion.
[6] J. Jacquinot et al., the JET Team, Overview of ITER physics deuterium–tritium experiments in JET, accepted for publication in Nucl. Fusion.
[7] A. Gibson, the JET Team, Phys. Plasmas 5 (1998) 1839.
[8] P. Andrew et al., these proceedings.
[9] JET Team (presented by P. Lomas), Proceedings of the 16th International Conference on Fusion Energy, Montreal, Canada, 1996 (IAEA, Vienna), Fusion Energy 2 (1997) 239.
[10] H. Guo et al., these proceedings.
[11] S. Sharapov et al., Stability of alpha particle driven Alfven eigenmodes in high performance JET D–T plasmas, accepted for publication in Nucl. Fusion.
[12] P.R. Thomas et al., Phys. Rev. Lett. 80 (1998) 5548.
[13] B.J.D. Tubbing et al., Nucl. Fusion 31 (1991) 839.
[14] M. Hugon et al., Nucl. Fusion 32 (1992) 33.
[15] F.M. Levington et al., Phys. Rev. Lett. 75 (1995) 4417.
[16] E.J. Strait et al., Phys. Rev. Lett 75 (1995) 4421.
[17] K. Ushigusa, the JT-60 Team, Proceedings of the 16th International Conference on Fusion Energy Montreal, Canada, 1996 (IAEA, Vienna) Fusion Energy 1 (1997) 37.
[18] The JET Team (presented by F.X. Soldner), Plasma Phys. Control. Fusion 39 (1997) B353.
[19] C. Gormezano et al., Phys. Rev. Lett. 80 (1998) 5544.
[20] V. Parail et al., Predictive Modelling of JET Optimised Shear Discharges, accepted for publication in Nucl. Fusion.
[21] W. Kerner et al., J. Comput. Phys. 142 (1998) 271.
[22] D.F.H. Start et al., Phys. Rev. Lett. 80 (1998) 4681.
[23] D.F.H. Start et al., in: Europhysics Conference Abstracts Proc. of the 24th EPS Conference on Controlled Fusion and Plasma Physics, Berchtesgaden, Germany, vol. 21A, 1997, part 1, 141.
[24] T. Takizuka et al., Proceedings of the 16th International Conference on Fusion Energy, Montreal, Canada, 1996 (IAEA, Vienna), Fusion Energy 2 (1997) 795.
[25] The JET Team (presented by M. Keilhacker), Plasma Phys. Control. Fusion 39 (1997) B1.
[26] H. Lingertat et al., these proceedings.
[27] F. Wagner et al., in Controlled Fusion and Plasma Heating (Proc. 17th Eur. Conf. Amsterdam, 1990), vol. 14B, part I, EPS Geneva (1990) 58.
[28] D.P. Schissel et al., Nucl. Fusion 29 (1989) 185.
[29] M. Kikuchi et al., in: Plasma Physics and Controlled Nuclear Fusion Research (Proc. 14th Int. Conf. Wurzburg 1992) vol. I. IAEA Vienna (1993) 189.
[30] F. Tibone et al., Nucl. Fusion 33 (1993) 1319.
[31] S.D. Scott et al., Proceedings of the 16th International Conference on Fusion Energy Montreal, Canada, 1996 (IAEA, Vienna), Fusion Energy 1 (1997) 573.

[32] M. Greenwald et al., Europhysics Conference Abstracts (Proc. of the 24th EPS Conference on Controlled Fusion and Plasma Physics, Berchtesgaden, Germany, 1997), vol. 21A, part 2, 569.
[33] M. Greenwald et al., Nucl. Fusion 28 (1988) 2199.
[34] A. Rolfe, The exchange of JET divertor modules using remote handling techniques, Proce. IEEE Int. Conf. on Robotics and Automation, May 1998, published on CD: ISBN 0-7803-4758-7.